RESEARCH ARTICLE Indian Journal of Animal Research, Volume 60 Special Issue: 60-67 (2026)

Effect of Sun's Bushen Huayu Formula on Endometrial Repair in a Thin Endometrium Model *via* Dual Modulation of the VEGF/Angiotensin II Axis and the DLL4/Notch1 Pathway

Yanfeng Liao[1], Feiyan Lian[1], Lihui Chen[1], Hongqing Zhang[1]

10.18805/IJAR.BF-2142

ABSTRACT

Background: The thin endometrium (TE) is a serious threat to female reproductive health and there are few effective treatment options. The Sun's Bushen Huayu Formula (BSHYF), a traditional Chinese medicine compound, has demonstrated efficacy in treating gynecological disorders, however, the effects of BSHYF on endometrial regeneration need to be systematically explored. **Methods:** The female SD rats with synchronized estrous cycles were used to establish a TE model and then the BSHYF intervention was performed. The major methodologies consisted of vaginal cytology in order to determine the estrous stage, histology to assess endometrial architecture and immunohistochemistry, qRT-PCR and western blot to analyze molecular pathways. **Result:** BSHYF treatment effectively ameliorated TE-induced uterine atrophy and metabolic disturbance, as evidenced by recovery of uterine structure and body weight. The histopathological and immunohistochemical findings showed that BSHYF-induced regeneration of endometrial layers, increased glandular density and upregulated Ang II and VEGF expression. Genes and protein-level analyses indicated that BSHYF stimulated the DLL4/Notch1 signaling pathway, which is essential in the process of vascular remodeling and endometrial repair. The current research has determined that BSHYF is an encouraging therapeutic agent in treating TE by modulating the VEGF/Ang II and DLL4/Notch1 pathways. The results give a mechanistic understanding of the effectiveness of BSHYF in endometrial regeneration.

Key words: DLL4/Notch1 pathway, Endometrial regeneration, Sun's bushen huayu formula, Thin endometrium, VEGF/Angiotensin II pathway.

INTRODUCTION

The endometrium, an important part of the female reproductive system, proliferates, differentiates and sheds in a cyclic manner when regulated by specific hormones and coordinated by molecular networks. The normal thickness of endometrium and the architecture of its functional layer are required for embryo implantation. Thin endometrium (TE) has become a major etiological factor in female infertility and recurrent miscarriage, defined as a pathological process that involves damage to the basal layer, sparse glands and decreased vascular density (Saad-Naguib *et al.*, 2023). Although not all infertility patients have endometrial thinning, the prevalence of endometrial thinning increases significantly in patients with a history of repeated intrauterine procedures or chronic endometritis. Regardless of the improvement in technologies and therapies, there is still variation between individuals and long-term hormone treatment in certain patients can increase the risk of thrombosis. These clinical issues justify the need to explore the molecular pathology of TE in order to formulate effective treatment strategies.

The recent research has clarified the close association between the endometrial regenerative potential and the local angiogenic microenvironments (Guo *et al.*, 2022). Vascular Endothelial Growth Factor (VEGF) is a master regulator of angiogenesis which causes proliferation, migration and invasion of endothelial cells through VEGFR2 activation, which plays a key role in endometrium repair (Ye *et al.*, 2019). Angiotensin II (Ang II), an important effector of the renin-angiotensin system, induces VEGF secretion by triggering AT1 receptors to form a two-factor control network (Butcher *et al.*, 2026). It is worth noting that angiogenic dysfunction is considered a key pathological aspect of TE and downregulation of VEGF and Ang II is related to spiral artery dysplasia and inadequate perfusion in the female reproductive system (Lei *et al.*, 2021; Zanon *et al.*, 2024). Nevertheless, there are still some gaps in the knowledge

[1]Department of Obstetrics and Gynecology, Fuzhou Hospital of Traditional Chinese Medicine Affiliated to Fujian University of Traditional Chinese Medicine, Fuzhou 350001, China.

Corresponding Authors: Yanfeng Liao and Hongqing Zhang; Department of Obstetrics and Gynecology, Fuzhou Hospital of Traditional Chinese Medicine Affiliated to Fujian University of Traditional Chinese Medicine, Fuzhou 350001, China.
Email: 15860818646@163.com; 18850669087@163.com

How to cite this article: Liao, Y., Lian, F., Chen, L. and Zhang, H. (2026). Effect of Sun's Bushen Huayu Formula on Endometrial Repair in a Thin Endometrium Model *via* Dual Modulation of the VEGF/Angiotensin II Axis and the DLL4/Notch1 Pathway. *Indian Journal of Animal Research.* **60(Special issue):** 52-29. doi: 10.18805/IJAR.BF-2142.

Submitted: 07-05-2026 **Accepted:** 07-07-2026 **Online:** 23-07-2026

of multifactor interactions and upstream signaling cascades that prevent the overall insight into the pathogenesis of TE. Delta-like ligand 4 (DLL4), a ligand of the Notch pathway, interacts with its receptor Notch1 to induce γ-secretase-mediated release of intracellular domain that will affect the expression of target genes (Joshi *et al.*, 2024). The DLL4/Notch1 axis in physiological angiogenesis controls proper vascular branching by negatively regulating proliferation of endothelial cells (Ke *et al.*, 2024). It was shown by Muley *et al.* that this pathway could be abnormally activated in the reproductive system to interfere with vascular maturity (Muley *et al.*, 2022). Subsequent work by Lv *et al.*, 2019 however, showed that the abnormal DLL4/Notch1 signaling in endometrial stromal cells interferes with paracrine cross-talk between endothelial cells, but its regulatory function in TE is not characterized. All these results imply that the TE pathogenesis can be due to dysregulation of angiogenic factors and the DLL4/Notch1 pathway.

Over the years, Traditional Chinese Medicine (TCM) has gained much experience in treating gynecological diseases and is also positively impacted by the multi-target nature and low toxicity of TCM preparations. TCM uses a holistic approach to therapy, which involves synergistic relationships between bioactive components in order to provide overall systemic regulation, improve metabolic homeostasis, hormonal balance and immune control (Qin *et al.*, 2023). In the TCM theory of the relationship between the kidneys and reproduction, it is proposed that a female should possess sufficient kidney essence stores and have a normal blood flow to ensure reproductive health and that TE is pathologically associated with insufficient kidney function (kidney vacuity) and impaired blood flow (blood stasis) (Hyun *et al.*, 2024; Shi *et al.*, 2024). Sun's Bushen Huayu formula (BSHYF), a classical prescription for "kidney deficiency with blood stasis syndrome", integrates 10 herbal components-*Human placenta*, *Cornu cervi degelatinatum*, *Fructus lycii*, *Morindae officinalis radix*, *Polygonati rhizoma*, *Cyathulae radix*, *Salviae miltiorrhizae radix*, *Paeoniae radix rubra*, *Angelicae sinensis radix* and *Rehmanniae radix*-based on the therapeutic principle of "tonifying kidney essence and activating blood circulation". Modern pharmacological studies reveal that BSHYF components exhibit estrogenic activity, anti-inflammatory, antioxidant and immunoregulatory properties (Fan *et al.*, 2024; Liu *et al.*, 2023; Liu *et al.*, 2024; Mehallah *et al.*, 2024; Sam-Ang *et al.*, 2023; Wang *et al.*, 2023; Yang *et al.*, 2022; Yang *et al.*, 2023; Zhang *et al.*, 2024). It is important to note that (Zhang *et al.*, 2024) showed that Salviae miltiorrhizae radix has strong antioxidative ability which protects endometrial integrity. Nevertheless, he mechanism by which BSHYF regulates the VEGF/Ang II and DLL4/Notch1 pathways in TE remains elusive (Oh *et al.*, 2025).

Conclusively, this paper explores TE pathogenesis in an organized manner and assesses the therapeutic effectiveness of BSHYF in order to explain the cross-talk between the VEGF/Ang II axis and DLL4/Notch1 pathway. We aim to enhance the position of TCM within assisted reproductive technologies, which eventually will lead to better endometrial receptivity.

MATERIALS AND METHODS

The experiment was conducted from January 2025 to March 2026 at Fuzhou Hospital of Traditional Chinese Medicine Affiliated to Fujian University of Traditional Chinese Medicine.

Composition and preparation of BSHYF

BSHYF integrates 10 medicinal components: *Human placenta* (Zi He Che, 6 g, Homo sapiens L. placenta [Hominidae]), *Cornu cervi degelatinatum* (12 g, Cervus nippon temminck antler [Cervidae]), *Fructus lycii* (15 g, Lycium barbarum L. [Solanaceae]), *Morindae officinalis radix* (15 g, Morinda officinalis How [Rubiaceae]), *Polygonati rhizoma* (12 g, Polygonatum sibiricum (L.) [Liliaceae]), *Cyathulae radix* (9 g, Achyranthes bidentata blume [Amaranthaceae]), *Salviae miltiorrhizae radix* (12 g, Salvia miltiorrhiza bunge [Lamiaceae]), *Paeoniae radix rubra* (9 g, Paeonia lactiflora Pall. [Ranunculaceae]), *Angelicae sinensis radix* (9 g, Angelica sinensis (Oliv.) Diels [Apiaceae]) and *Rehmanniae radix* (12 g, Rehmannia glutinosa (Gaertn.) DC. [Orobanchaceae]). All raw materials identified by macroscopic and microscopic pharmacognostic analysis by qualified people at Fuzhou Hospital of Traditional Chinese Medicine (Fuzhou, China) were extracted three times using reflux boiling (1:8 w/v aqueous solvent, 60 min per cycle). The combined filtrates were vacuum-extracted to give a standardized extract (total 4g crude drug/mL) that was filtered through a 0.22 μm membrane filter to be sterilized and kept at 4°C. To get the 2.16, 4.32 and 8.64 g/kg dose formulations to be administered in vivo, the stock solution was diluted with sterile distilled water.

Animal and group

The study was conducted on 36 female Sprague-Dawley rats (8-10 weeks old, 200±20 g) purchased from Sibeifu Biotechnology Co., Ltd. (SCXK [Su] 2022-0006, Suzhou, China) housed in controlled conditions (22±1°C, a 12-hour light/dark cycle). The Animal Care and Use Committee of Fujian University of Traditional Chinese Medicine has assessed and approved all the experimental protocols that include animals (Approval No. IACUC FJABR 2023073001). All research is done in accordance with the ethical principles of the CPCSEA regarding the welfare of animals. Operations were carried out in a humane way, with proper anesthesia to reduce animal discomfort and post-operative pain relief was given when necessary.

The rats were randomly divided into five experimental groups: Control group (n = 9), Model group (n = 9), low (L, n = 6), medium (M, n = 6) and high (H, n = 6) doses of BSHYF.

Experimental model establishment

Experimental protocol used in the model induction was initiated by oral feeding of hydroxyurea (450 mg/kg, cat. no.

MB1307, Meilunbio, Dalian, Liaoning, China) on 10 consecutive days of the estrous period. After the last dose of hydroxyurea, animals were given intravenous injection of 5 mL/kg of 10% high-molecular dextran (Mw 800,000, cat. no. 61217ES, Yeasen Biotechnology (Co., Ltd., Shanghai, China). The Control group rats received injection of 5 mL/kg of saline. The signs of renal deficiency and blood stasis were the presence of fur dullness, body weight loss and ear, paw and tail discoloration to dark purple. This was followed by surgical intervention to create thin endometrial model in the estrous phase. During the estrus period, perform an open abdominal surgery to expose both uterine horns. Slowly inject 0.5 mL of 95% ethanol into the cavity of each uterine horn using a syringe. Retain the solution for 5 minutes, then repeatedly aspirate and irrigate or rinse with normal saline to remove residual ethanol, followed by suturing the abdominal cavity. Rats in the Control group were subjected to sham surgery, whereas rats in the Model group received saline and rats in the BSHYF (L, M, H) group received daily oral administration of BSHYF throughout 20 days. Rats were euthanized by intraperitoneal injection of pentobarbital sodium (50 mg/kg, cat. no. P3761, Sigma-Aldrich, St. Louis, MO, USA).

Giemsa staining

The cell fixation was carried out by fixing cells in anhydrous methanol (cat. no. 589596, Sigma-Aldrich, St. Louis, MO, USA) at room temperature for 5 minutes. The slides were then stained using 10% Giemsa working solution diluted in phosphate buffered saline after 20 minutes incubation at 21±1°C in a light-protected environment. Dehydration procedures were done with three consecutive 30 seconds baths of 70, 90 and absolute ethanol and cleared with xylene (cat. no. 534056, histological grade, Sigma-Aldrich, St. Louis, MO, USA; 2×2 min). The Permount synthetic resin (cat. no. SP15-500, Thermo Fisher Scientific, Waltham, MA, USA) was used as permanent mounting and cellular architecture was assessed by bright-field microscopy (Olympus BX53, Olympus Corporation, Tokyo, Japan) at 200× oil-immersion optics.

Hematoxylin and eosin (H and E) staining

The formalin-fixed paraffin-embedded tissue blocks were cut at 5 µm thick section on the rotary microtome. Triple xylene immersion (5 min each) followed by sequential ethanol rehydration (100%-70%) was used in deparaffinization. The nuclei were stained by exposing them to Harris hematoxylin (cat. no. 6765001 or equivalent non-acidified, Epredia, Kalamazoo, MI, USA) for 8 minutes and then to tap water (blueing) for 5 minutes. Counterstaining of cytoplasm was done using 0.5 percent eosin Y solution (Sigma-Aldrich, St. Louis, MO, USA) for 120 seconds with continuous agitation. The sections mounted with neutral balsam (cat. no. G8590, Solarbio Science and Technology Co., Ltd., Beijing, China) were examined thoroughly with the help of a Nikon E200 microscope (Nikon Corporation, Tokyo, Japan) at 200×.

Immunohistochemistry (IHC)

Paraffin-embedded endometrial sections were deparaffinized, rehydrated and then antigen retrieval was performed with citrate buffer (cat. no. P0081, Beyotime Biotechnology, Shanghai, China). Endogenous peroxidase activity was quenched using 3 per cent hydrogen peroxide and nonspecific binding was inhibited using 5% bovine serum albumin (cat. no. ST2249, Beyotime Biotechnology, Shanghai, China). The sections were incubated at 4°C overnight with the primary antibodies to VEGF (1:500, cat. no. 66828-1-Ig, Proteintech Group, Inc., Wuhan, Hubei, China) and Ang II (1:100, cat. no. H-002-12, Phoenix Pharmaceuticals, Inc., Burlingame, CA, USA). Following 1 hour incubation with HRP-conjugated secondary antibody (1:500, cat. no. SA00001-2, Proteintech Group, Inc., Wuhan, Hubei, China) at 21°C, the sections were washed three times with PBS. The immunoreactivity was developed using the 3,3 diaminobenzidine substrate (cat. no. PR30018, Proteintech Group, Inc., Wuhan, Hubei, China) and the nuclei were counterstained by hematoxylin and observed under a bright-field microscope (Nikon Eclipse E100, Nikon Corporation, Tokyo, Japan).

Quantitative real-time PCR (qRT-PCR)

The experimental procedures were performed as described previously (Yaseen *et al.*, 2025). The extraction of total RNA of endometrial tissues was performed with TRIzol reagent (cat. no. 15596026, Invitrogen, Thermo Fisher Scientific, Waltham, MA, USA) and DNase I (cat. no. MD80101, Magen Biotechnology Co., Ltd., Guangzhou, Guangdong, China), then cDNA was synthesized through reverse transcription. On an ABI 7300 system quantitative PCR used SYBR Green Supermix (cat. no. S2024L, US Everbright Inc., Suzhou, Jiangsu, China) as a thermal cycle (95°C (5 min) with subsequent 40 cycles of 95°C (20 s) and 56°C (20 s) and finally 72°C (38 s) and dissociation curve analysis. The primer sequences (Table 1) of DLL4, Notch1, VEGF, AGT and GAPDH were purchased from

Table 1: Sequences for qRT-PCR.

Gene	Primer	Sequence (5′-3′)
DLL4	Forward	ACAAGAATAGCGGCAGTGGT
	Reverse	TTCTTACCCACAGCAAGGGAG
Notch1	Forward	CAGGCAACAGTGAGGAAGAAG
	Reverse	GCAGCATCTGAACGAGAGTATC
VEGF	Forward	TTACTGCTGTACCTCCACCAT
	Reverse	CAGGACGGCTTGAAGATATACTC
AGT	Forward	GGCATCTACACGCTGACCTT
	Reverse	CCATCTTCCCGGTGTTGGAT
GAPDH	Forward	ACGGCAAGTTCAACGGCACAG
	Reverse	GAAGACGCCAGTAGACTCCACGAC

Shangya Biotech (Fuzhou, Fujian, China). GAPDH was used as reference to normalize relative mRNA expression using the $2^{-\Delta\Delta Ct}$ method.

Western blot

The experimental procedures were performed as described previously (Tabet *et al.*, 2025). The uterine tissue samples were homogenized in ice-cold RIPA lysis buffer (cat. no. MA0151, Meilunbio, Dalian, Liaoning, China). The denatured proteins (40 µg per lane) were separated by 8% SDS-PAGE gels (UE series, Suzhou UElandy Biotechnology Co., Ltd., Suzhou, Jiangsu, China). The proteins were transferred to PVDF membranes by wet transfer at 100V in Tris-glycine-methanol buffer, 70 minutes. The membranes were blocked with 5% non-fat milk (BBI Life Sciences, Shanghai, China) in TBST and incubated overnight at 4°C with primary antibodies: GAPDH (1:50,000, cat. no. 60004-1-Ig, Proteintech Group, Inc., Wuhan, Hubei, China), Notch1 (1:4,000, cat. no. 20687-1-AP, Proteintech Group, Inc., Wuhan, Hubei, China) and DLL4 (1:8,000, cat. no. 21584-1-AP, Proteintech Group, Inc., Wuhan, Hubei, China). HRP-conjugated secondary antibodies (cat. no. SA00001-1 with mouse, SA00001-2 with rabbit, Proteintech Group, Inc., Wuhan, Hubei, China) were used for 1 hour at room temperature. The protein bands were detected with ECL reagent on a TOUCH IMAGER XLI system. The intensity of the bands was measured by ImageJ program (National Institutes of Health, Bethesda, MD, USA).

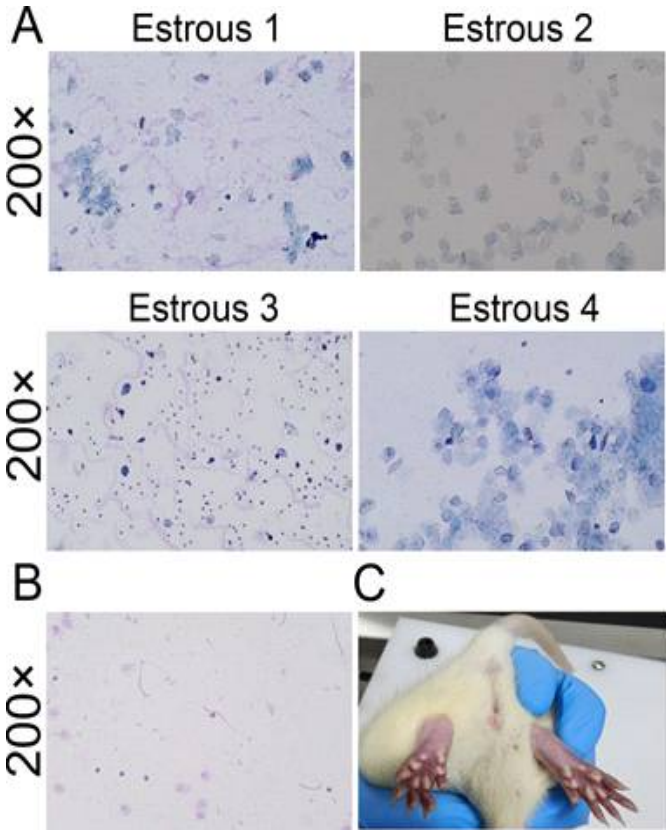
Statistical analysis

The results are represented as mean±standard deviation and were processed through the help of SPSS 26.0 software (IBM Corporation, Armonk, NY, USA). The comparison of the groups was conducted through one-way ANOVA with a post hoc test using the Tukey method. The P-value of less than 0.05 was used to indicate statistical significance. The investigators were blinded to group allocation throughout the process of data gathering and processing.

RESULTS AND DISCUSSION

Estrous cycle synchronization and pregnancy confirmation

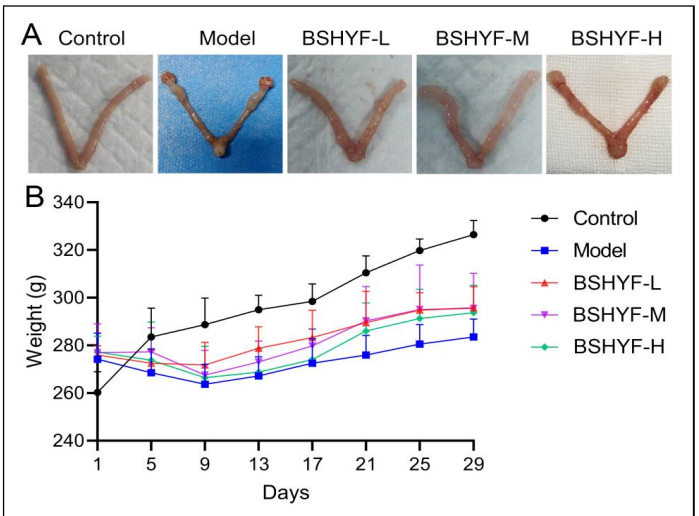
In order to obtain a stable reproductive model of female SD rats, we first ascertained regular estrous cycles through



(A) Representative images of vaginal smear cytology stained with Giemsa for estrous cycle staging. (B) Representative images of vaginal plugs and spermatozoa in vaginal smears confirming successful mating. (C) Macroscopic view of hind limb deep purple discoloration indicating successful TE model establishment.

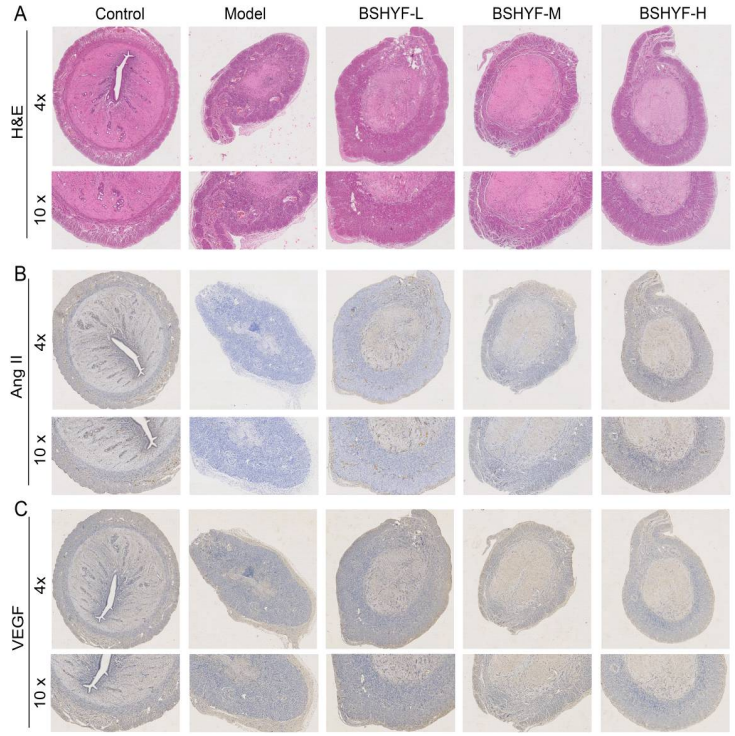
Fig 1: Estrous cycle synchronization and pregnancy confirmation.

daily monitoring of vaginal smears by Giemsa staining during four consecutive cycles (Fig 1A). The next step was to perform TE modeling on selected female rats during the estrus stage, which was followed by a 20-day BSHYF treatment regimen. Upon completion of the treatment regimen, suitable rats were co-housed with male rats at a



(A) Photographs of uterine tissue. (B) Line graph depicting longitudinal body weight changes from gestational day 1 to endpoint.

Fig 2: Effects of BSHYF on uterine morphology and body weight in TE rats.



(A) H and E staining illustrates the effects of BSHYF treatment on tissue architecture in TE model rats. (B) Immunohistochemical analysis of Ang II expression in TE model rats following BSHYF treatment. (C) Immunohistochemical analysis of VEGF expression in TE model rats following BSHYF treatment.

Fig 3: Histopathological restoration of endometrial structure by BSHYF.

1:1 ratio during the estrus stage and evidence of successful mating was ensured by the observation of vaginal plug or spermatozoa in vaginal smears on day 1 of gestation (Fig 1B). Deep purple discoloration of the hind limb (Fig 1C) was used to confirm the exact timing of the gestational window and the uniformity of the model formation.

BSHYF ameliorates TE-related uterine atrophy and metabolic dysfunction

The longitudinal monitoring identified considerable physiological changes of the TE model. The model group had significantly lower uterine volume, atrophic morphology and much thinner uterus walls than the control group. Such abnormalities were partially corrected by BSHYF treatment, especially in the BSHYF high-dose group (Fig 2A). Beginning on day 5 after modeling, the model group experienced a significant decrease in body weight which lasted up to the end of the experiment. The effect of BSHYF intervention on body weight was found to be partial in low-, medium- and high-dose groups, without any dose-dependent differences detected implying that BSHYF intervention recovers metabolic functions (Fig 2B). These findings suggest that BSHYF is effective in reducing the impact of metabolic stress and improving reproductive potential in pathological models.

BSHYF restores endometrial histopathological architecture

The HE staining revealed several important structural abnormalities in the TE model: The model group showed marked thinning of both functional and basal endometrial layers and had glandular atrophy (abnormal branching and poor distribution) and diffuse inflammatory infiltration (Fig 3A). IHC analysis revealed suppressed expression of Ang II and VEGF in the TE model, which was strongly reversed by BSHYF, especially in the high-dose group. This information clarifies the function of BSHYF in reversing the endometrial atrophy and normalizing vascular dysplasia.

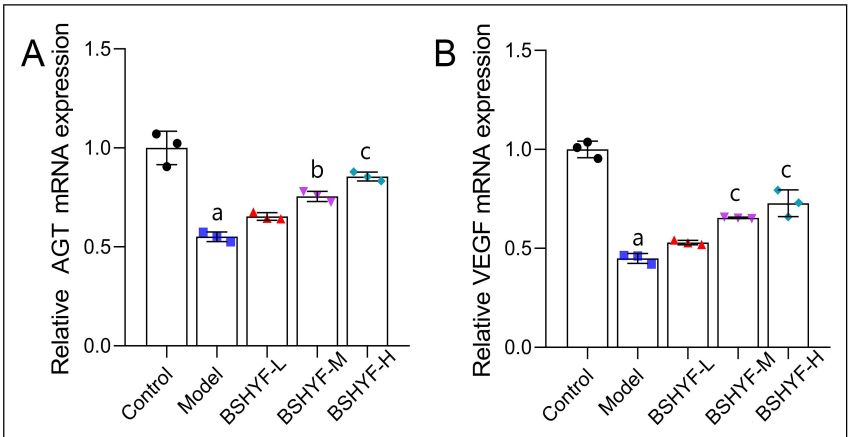
BSHYF upregulates angiogenesis-related regulatory factors

qRT-PCR analysis indicated that mRNA levels of AGT (as an upstream indicator of local renin-angiotensin system activity leading to Ang II production) and VEGF were markedly down-regulated in the TE model rat group relative to the controls. Whereas low-dose BSHYF did not affect their expression, medium- and high-dose BSHYF greatly increased both transcripts (Fig 4A, B) as predicted by the IHC observations.

BSHYF activates the DLL4/Notch1 pathway for endometrial regeneration

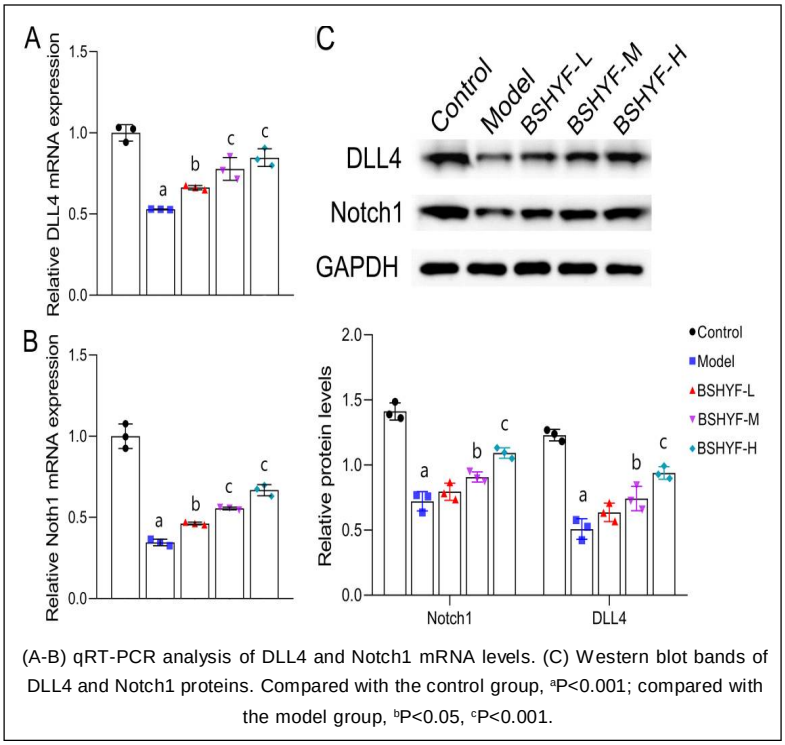
Subsequent experiments clarified the molecular process of endometrial repair. In the TE model group, both gene and protein levels of DLL4 and Notch1 were decreased, but BSHYF intervention restored this suppression and the effect was most noticeable at the highest dose of BSHYF (Fig 5A-C). Taken together, these results point to the role of BSHYF in inducing endometrial regeneration through the regulation of the DLL4/Notch1 signaling pathway.

Our study demonstrates that BSHYF effectively ameliorates TE in a rat model by restoring uterine morphology (Fig 2A), reversing weight loss (Fig 2B) and rebuilding histopathological architecture (Fig 3A). These structural improvements are tightly coupled with angiogenic reactivation. Immunohistochemistry (Fig 3B-C) and qRT PCR (Fig 4A, 4B) revealed that TE induced suppression of Ang II and VEGF proteins and their transcripts (AGT and VEGF) was reversed by BSHYF in a dose dependent manner, with high dose treatment restoring mRNA levels to 75 85% of control values. The parallel recovery of glandular density (Fig 3A) suggests that BSHYF mediated angiogenic signaling directly supports epithelial regeneration (Ye *et al.*, 2019).



(A) qRT-PCR showing *AGT* mRNA levels. (B) qRT-PCR showing *VEGF* mRNA levels. Compared with the control group, $^{a}P<0.001$; compared with the model group, $^{b}P<0.01$, $^{c}P < 0.001$.

Fig 4: qRT-PCR validation of angiogenesis-related transcripts.



(A-B) qRT-PCR analysis of DLL4 and Notch1 mRNA levels. (C) Western blot bands of DLL4 and Notch1 proteins. Compared with the control group, [a]P<0.001; compared with the model group, [b]P<0.05, [c]P<0.001.

Fig 5: Activation of the DLL4/Notch1 pathway by BSHYF intervention.

Beyond promoting vessel formation, BSHYF also reactivates the DLL4/Notch1 pathway (Fig 5A-C), which serves as a critical brake to prevent aberrant sprouting (Ke *et al.*, 2024; Shaw *et al.*, 2024). Notably, DLL4/Notch1 upregulation exceeded that of VEGF after high dose treatment, implying a preferential activation of maturation signals. The orderly glandular architecture observed in treated groups (Fig 3A) further supports a balanced angiogenic program, VEGF/Ang II drives initial growth while DLL4/Notch1 ensures proper patterning and functional integrity.

The correlative nature of our data does not permit causal conclusions; however, the dose dependent responses across both pathways support a specific pharmacological effect. Whether DLL4/Notch1 activation is downstream of VEGF or an independent axis requires future inhibitor studies. Systemically, BSHYF partially rescued TE induced weight loss (Fig 2B) without a clear dose response, suggesting distinct mechanisms from local angiogenic effects, possibly involving anti inflammatory actions of herbal components (Liu *et al.*, 2024; Wu *et al.*, 2023).

CONCLUSION

In summary, BSHYF restores endometrial structure and systemic metabolism in TE rats through coordinated upregulation of the VEGF/Ang II axis and DLL4/Notch1 pathway. This dual, balanced angiogenic modulation distinguishes BSHYF from conventional therapies and provides a mechanistic foundation for its clinical application in endometrial repair.

Funding

This study was supported by Natural Science Foundation of Fujian Provincial Department of Science and Technology (grant no. 2023J011559).

Data availability

Data are available from the corresponding author upon reasonable request.

Author contributions

Conceptualization: YanFeng Liao, Hongqing Zhang; Data curation: YanFeng Liao; Funding acquisition: YanFeng Liao; Investigation: YanFeng Liao, Feiyan Lian; Software: Lihui Chen; Visualization: YanFeng Liao, Feiyan Lian, Lihui Chen; Writing-original draft: YanFeng Liao, Hongqing Zhang; Writing-review and editing: YanFeng Liao, Hongqing Zhang.

Conflict of interest

The authors declare no conflict of interest.

REFERENCES

Butcher, D.R., Parris, C.N., Crichton, S.J. *et al.* (2026). Unlocking the potential of targeting the angiotensin II type 1 receptor in cancer. *Oncogene*. **45(4):** 479-490.

Fan, Z., Liu, J. and Wang, X. *et al.* (2024). Paeoniae Radix Rubra: A review of ethnopharmacology, phytochemistry, pharmacological activities, therapeutic mechanism for blood stasis syndrome and quality control. *Chem Biodivers*. **21:** e202401119.

Guo, Q., Chang, Y., Li, J. *et al.* (2022). Regenerative effects of locally or intra-arterially administered bmscs on the thin endometrium. *Front Bioeng Biotechnol*. **10:** 735465.

Hyun, J.Y., Jung, H.S. and Park, J.Y. (2024). Herbal therapeutics for female infertility: A systematic review and meta-analysis. *J. Ethnopharmacol*. **319:** 117258.

Joshi, D., Coon, B.G., Chakraborty, R. *et al.* (2024). Gamma protocadherins in vascular endothelial cells inhibit Klf2/4 to promote atherosclerosis. bioRxiv [Preprint]. 01.16.575958.

Ke, X., Xia, S., Yu, W. *et al.* (2024). Delta like 4 regulates cerebrovascular development and endothelial integrity *via* DLL4-NOTCH-CLDN5 pathway and is vulnerable to neonatal hyperoxia. *J Physiol*. **602:** 2265-2285.

Lei, L., Lv., Q, Jin, Y. *et al.* (2021). Angiogenic microspheres for the treatment of a thin endometrium. *ACS Biomater Sci. Eng*. **7:** 4914-4920.

Liu, L., Jiao, Y., Yang M. *et al.* (2023). Network pharmacology, molecular docking and molecular dynamics to explore the potential immunomodulatory mechanisms of deer antler. *Int. J. Mol. Sci*. 24.

Liu, R., Zhang, X., Cai, Y. *et al.* (2024). Research progress on medicinal components and pharmacological activities of polygonatum sibiricum. *J. Ethnopharmacol.* **328:** 118024.

Lv, H., Nan, Z., Jiang, P. *et al.* (2019) Vascular endothelial growth factor 165 inhibits pro-fibrotic differentiation of stromal cells *via* the DLL4/Notch4/smad7 pathway. *Cell Death Dis*. **10:** 681.

Mehallah, H., Djebli, N., Ngoc Khanh, P. *et al.* (2024). In silico and *in vivo* study of anti-inflammatory activity of Morinda longissima (*Rubiaceae*) extract and phytochemicals for treatment of inflammation-mediated diseases. *J. Ethnopharmacol*. **328:** 118051.

Muley, A., Kim, Uh M., Salazar-De Simone, G. *et al.* (2022). Unique functions for Notch4 in murine embryonic lymphangiogenesis. *Angiogenesis*. **25(2):** 205-224.

Oh, J.M., Choi, D.Y. and Kim H.S. (2025) Persistent stimulation of sex-related hormones in the uterus is associated with differences in the Igf/Akt signaling pathway and uterine damage. *Indian Journal of Animal Research*. **59(4):** 574-580. doi: 10.18805/IJAR.BF-1886.

Qin, X., Sun, K., Ao, Y. *et al.* (2023). Traditional Chinese medicine for frozen shoulder: An evidence-based guideline. *J. Evid. Based Med*. **16:** 246-258.

Rodriguez-Eguren, A., Bueno-Fernandez, C., Gomez-Alvarez, M. *et al.* (2023). Evolution of biotechnological advances and regenerative therapies for endometrial disorders: A systematic review. *Hum Reprod Update*. **30:** 584-613.

Saad-Naguib, M.H., Kenfack, Y., Sherman, L.S. *et al.* (2023). Impaired receptivity of thin endometrium: Therapeutic potential of mesenchymal stem cells. *Front Endocrinol (Lausanne).* **14:** 1268990.

Sam-Ang, P., Phanumartwiwath, A., Liana, D. *et al.* (2023). UHPLC-QQQ-MS and RP-HPLC detection of bioactive alizarin and scopoletin metabolites from morinda citrifolia root extracts and their antitubercular, antibacterial and antioxidant activities. *ACS Omega*. **8:** 29615-29624.

Shaw, P., Dwivedi, S.K.D., Bhattacharya, R. *et al.* (2024). VEGF signaling: Role in angiogenesis and beyond. *Biochim Biophys Acta Rev Cancer*. **1879:** 189079.

Shi, Y.X., Xu, L., Wang, X. *et al.* (2024). Paris polyphylla ethanol extract and polyphyllin I ameliorate adenomyosis by inhibiting epithelial-mesenchymal transition. *Phytomedicine.* **127:** 155461.

Tabet, K., Dahou, A.A., Tahlaiti, H. *et al.* (2025). Assessment of the probiotic and technological potential of three strains of *lactobacillus acidophilus* isolated from local dairy products from western algeria. *Asian Journal of Dairy and Food Research.* doi: 10.18805/ajdfr.DRF-530.

Wang, T., Li, Y.Q., Yu, L.P. *et al.* (2023). Compatibility of polygonati rhizoma and angelicae sinensis radix enhance the alleviation of metabolic dysfunction-associated fatty liver disease by promoting fatty acid beta-oxidation. *Biomed Pharmacother.* **162:** 114584.

Wu, M., Lai, H., Peng, W. *et al.* (2023). Monotropein: A comprehensive review of bios ynthesis, physicochemical properties, pharmacokinetics and pharmacology. *Front Pharmacol*. **14:** 1109940.

Yang, L.F., Teng, L., Huang, Y.H. *et al.* (2022). Undescribed ecdysteroids and phenolic glycosides from the roots of Cyathula officinalis Kuan and their anti-inflammatory activity in LPS-induced RAW 264.7 macrophages *in vitro*. *Phytochemistry*. **196:** 113101.

Yang, Y., Wang, Y., Deng, Y. *et al.* (2023). Fructus lycii and salvia miltiorrhiza bunge extract attenuate oxidative stress-induced photoreceptor ferroptosis in retinitis pigmentosa. *Biomed Pharmacother*. **167:** 115547.

Yaseen Tareq Farah, Al-Jumaily Kh, M. (2025). The impact of Interleukin-21 and 23 serum level and gene expression in celiac disease among sample of iraqi patients. *Asian Journal of Dairy and Food Research*. **44(2):** 234-239. doi: 10.18805/ajdfr.DRF-476.

Ye, Q., Zhang, Y., Fu, J. *et al.* (2019). Effect of ligustrazine on endometrium injury of thin endometrium rats. *Evid Based Complement Alternat Med*. 7161906.

Zanon, P., Terraciano, P.B., Quandt, L. *et al.* (2024). Angiotensin II - AT1 receptor signalling regulates the plasminogen-plasmin system in human stromal endometrial cells increasing extracellular matrix degradation, cell migration and inducing a proinflammatory profile. *Biochem Pharmacol.* **225:** 116280.

Zhang, Y., Jia, K., Li, Y. *et al.* (2024). Rehmanniae radix praeparata aqueous extract improves hepatic ischemia/reperfusion injury by restoring intracellular iron homeostasis. *Chin. J. Nat Med*. **22:** 769-784.